HHS Public Access

Author manuscript

Nat Neurosci. Author manuscript; available in PMC 2014 August 01.

Published in final edited form as:

Nat Neurosci. 2014 February ; 17(2): 248–253. doi:10.1038/nn.3625.

Medial prefrontal D1 dopamine neurons control food intake

Benjamin B Land[1], **Nandakumar S Narayanan**[1,2], **Rong-Jian Liu**[1], **Carol A Gianessi**[1], **Catherine E Brayton**[1], **David Grimaldi**[1], **Maysa Sarhan**[1], **Douglas J Guarnieri**[1], **Karl Deisseroth**[3], **George K Aghajanian**[1], and **Ralph J Dileone**[1]

[1]Department of Psychiatry and Ribicoff Research Facilities, Yale University School of Medicine, New Haven, CT 06520

[2]Department of Neurology, Carver College of Medicine, University of Iowa, Iowa City, IA 52242

[3]Departments of Bioengineering and Psychiatry & Behavioral Sciences, Stanford University, Stanford, CA 94305

Abstract

Although the prefrontal cortex influences motivated behavior, its role in food intake remains unclear. Here, we demonstrate a role for D1-type dopamine receptor-expressing neurons in the medial prefrontal cortex (mPFC) in the regulation of feeding. Food intake increases activity in D1 neurons of the mPFC in mice, and optogenetic photostimulation of D1 neurons increases feeding. Conversely, inhibition of D1 neurons decreases intake. Stimulation-based mapping of prefrontal D1 neuron projections implicates the medial basolateral amygdala (mBLA) as a downstream target of these afferents. mBLA neurons activated by prefrontal D1 stimulation are CaMKII positive and closely juxtaposed to prefrontal D1 axon terminals. Finally, photostimulating these axons in the mBLA is sufficient to increase feeding, recapitulating the effects of mPFC D1 stimulation. These data describe a new circuit for top-down control of food intake.

The decision of whether or not to eat is critically important for the survival of an animal. For humans, the modern environment with ready access to food biases this decision and helps to contribute to overeating and obesity. In mammals, the prefrontal cortex (PFC) plays a crucial role in decision-making and regulation of behavior[1,2], and is implicated in control of food intake although the underlying neural mechanisms remain unclear. Humans with frontotemporal dementia display hyperphagia, whereas generalized dementia patients do not[3]. Additionally, human imaging studies have correlated activity in the PFC with both hunger in obese patients[4], as well as the pleasantness of food[5]. However, preclinical studies using lesions of the PFC have varied and opposing effects on intake[6–8], and many pharmacological manipulations targeting monoamine systems produce no change at all[9]. This disparity between human and preclinical studies suggests limitations in the classical

Author contributions: BBL, NSN, and RJD conceived the study; BBL NSN, RL, CAG and GA conducted the experiments and analyzed the data; CEB, DG, MS, DJG, and KD provided viral constructs and genotyping support; BBL, NSN, and RJD wrote the manuscript.

pharmacological and inactivation approaches, and that manipulation of specific cell types within the PFC is necessary to determine respective contributions to food intake.

Prefrontal dopamine systems represent an attractive target for neural influence over feeding behaviors. Midbrain dopaminergic projections play an important role in food intake, and without dopamine animals become hypophagic and die from starvation[10–12]. Both nigrostriatal and mesolimbic dopamine systems contribute to feeding[13–16], and dopaminergic neurons from the ventral tegmental area also prominently project to the PFC[17]. While dopaminergic systems in the prefrontal cortex are implicated in control over tasks such as working memory, habit, and timing[18–20], a direct effect of prefrontal dopamine systems in feeding remains unexplored.

Dopamine D1 receptors are highly expressed in the medial prefrontal cortex (mPFC)[21], and there is evidence that dopamine D1 receptor-containing neurons in the mPFC play a role in food-related behaviors[22,23]. However, direct assessment of food intake as a result of prefrontal D1 neuron stimulation has yet to be investigated. In the present study, we first demonstrate that mPFC D1 neurons are activated during feeding. We then use cell-type specific optogenetics to stimulate or inhibit mPFC neurons expressing D1 receptors and directly assess their influence on food intake.

RESULTS

D1-dopamine receptor neurons are activated during feeding

To map prefrontal dopamine circuitry related to feeding, we examined whether feeding activated prefrontal neurons. Mice expressing Cre recombinase in D1-dopamine receptor neurons (*Drd1a-cre*$^+$, see Supplemental Figure 1a) were food-deprived for 24 hours, and then tested for 90 min with free access to chow, in order to isolate a discrete feeding period. Animals that were deprived ate approximately 6-fold more than control *Drd1a-cre*$^+$ animals that remained *ad-lib* fed (n = 2,2 cage averages, control = 0.17± 0.04, deprived = 1.15± 0.20, mean ± s.e.m.). Immediately after feeding, animals were sacrificed and immunohistochemical analyses were performed. Compared to control animals, restricted mice showed significantly increased Fos density in the mPFC (Fig. 1a,b, P = 0.007). As D1-type dopamine receptors have higher expression in rodent medial prefrontal regions[21], we examined if neurons with increased feeding-related activity expressed D1 dopamine receptors by co-labeling with an antibody against Cre recombinase. Restricted animals showed a significant increase in the percentage of D1+ neurons that were also Fos+, indicating that these neurons were more active during feeding (Fig. 1c,d and Supplemental Figure 2, P = 0.022,). These results demonstrate that the activity of mPFC D1 neurons increases with feeding.

D1-selective PFC neuronal activation using light

To establish that we could selectively stimulate only prefrontal D1 neurons, we administered a virus containing a double-inverted flox channelrhodopsin construct (*AAV-EF1a-DIO-ChR2-eYFP*) into the mPFC of *Drd1a-cre*$^+$ mice[24] (Fig. 2a and Supplemental Figure 3 a,b). ChR2 was expressed predominantly in medium-sized pyramidal cells (Fig. 2b), and patch

clamp experiments on layer 5 D1-ChR2$^+$ neurons showed no I_h current at hyperpolarizing currents ("voltage sag", red arrow, Fig. 2c) and no rebound depolarization (blue arrow) as compared to larger, D1-negative pyramidal neurons within layer 5 (Supplemental Figure 3 c,d). This is consistent with previous descriptions of D1 pyramidal neurons in prefrontal cortex[25]. Photostimulation of the brain slice with 20 Hz, 473 nm light (frequencies based on preliminary behavioral tests) resulted in highly reliable, frequency-dependent inward currents in these neurons (Fig. 2d), which produced sustained action potentials for at least 3 min (Fig. 2e). These data demonstrate that we are able to selectively activate D1 neurons in the mPFC with high fidelity.

Unilateral activation of D1 PFC neurons drives intake

To assess whether D1-neuronal activation was sufficient to influence feeding, ChR2 was expressed in the left mPFC of *Drd1a-cre*$^+$ mice, and a fiberoptic cannula was implanted to allow for optical illumination during behavior (Fig. 3a). ChR2 expression in layer 5 was verified and photoillumination produced a robust Fos response compared to control, *Drd1a-cre*$^-$ animals, confirming neuronal activation *in vivo* (Fig. 3b, $P = 0.01$). Animals were habituated to a home cage containing grain pellets in a dish, available ad-libitum, for three days. Subsequent to habituation, animals were stimulated at 5 or 20 Hz (in 3 min on/off cycles), and the number of pellets consumed in an hour was recorded. *Drd1a-cre*$^+$ mice ate significantly more pellets than *Drd1a-cre*$^-$ controls when stimulated at 20 Hz, but not at 5 Hz (Fig. 3c, $P = 0.029$). Further, consumption of a highly palatable, high-fat chow (45%) was also significantly increased in *Drd1a-cre*$^+$ animals after 20-Hz photostimulation (Fig. 3d, $P = 0.032$).

Because these increases in feeding were observed during times when mice do not usually feed (mid-light cycle), we also used an operant paradigm to measure food intake during natural feeding periods. Animals were trained under food restriction to make a nose-poke ("response") for a grain pellet, and once trained, were re-fed until their weights were equal to or greater than pre-training weights. On the testing day, animals were returned to the test chamber before the onset of the dark cycle and coupled to the laser. Each hour, the animals went through two, 30-min epochs. In the first epoch there was no photostimulation ('no-light'), while in the second epoch illumination occurred in a 3-min on/off cycle at 20 Hz ('light', Fig. 3e). *Drd1a-cre*$^+$ animals significantly increased the number of pokes only during the 'light' epochs, compared to *Drd1a-cre*$^-$ littermates who are unaffected by illumination (Fig. 3f and Supplemental Figure 4a,b, $P = 0.025$). Within the 'light' epoch, there was no significant difference in responding when the laser was on versus when it was off, although there was a trend towards an increase (Supplemental Figure 4c,d, $P = 0.094$), suggesting that responses may not be absolutely time-locked to stimulation. Nonetheless, in total the *Drd1a-cre*$^+$ animals had significantly increased pokes during the 'light' epoch compared to the 'no-light' epoch (Fig. 3g, $P = 0.0003$). Comparing the ratio of 'light' vs. 'no-light' cumulative responses over each hour showed this increase in 'light' epoch responses to be sustained and linear over 13 hours (Fig. 3h, $P = 0.04$). *Drd1a-cre*$^+$ animals also ate more pellets than controls during this time (Fig. 3i; a total increase of ~1 g, $P = 0.049$), demonstrating that increased responding corresponded to an increase in intake and was not a non-specific motor response. Locomotor activity during the light epoch was

unchanged, showing that prefrontal D1 stimulation did not influence gross motor movement (Supplemental Figure 5a,b, $P = 0.77$). In addition, free overnight consumption of high-fat chow was significantly increased with photoactivation (Supplemental Figure 5c, $P = 0.045$), while stimulation did not significantly increase licking for water, suggesting this response is specific to food consummatory behavior (Supplemental Figure 5d, $P = 0.38$). Finally, nose-poking on an unreinforced port was decreased during photoactivation, suggesting that animals spent less time exploring the environment at times when feeding was increased (Supplemental Figure 5e, $P = 0.05$), consistent with limited effects of stimulation on non-specific motor activity. These results demonstrate that sustained photostimulation of prefrontal D1 neurons is sufficient to selectively drive food intake under sated conditions during normal feeding.

Bilateral inhibition of D1 PFC reduces intake

To test whether D1 prefrontal inhibition modifies intake, we expressed halorhodopsin (eNpHR 3.0, *AAV-EF1a-DIO-eNpHR3.0-EYFP*) bilaterally in D1 neurons of the mPFC, and implanted bilateral optical fiber cannula (Fig. 4a). To motivate consumption, animals were restricted to approximately 90% free-feeding body weight while being habituated to ad-lib grain pellets. After four days of habituation, animals were coupled to the laser and received 590 nm light during two, 15-min epochs in an hour-long test (Supplemental Figure 6a). During the illuminated epochs, *Drd1a-cre*$^{+}$ animals ate significantly fewer pellets than when the light was off ($P = 0.045$), compared to *Drd1a-cre*$^{-}$ animals, whose intake was unchanged by light (Fig. 4b and Supplemental Figure 6a). Total intake between the groups was not different (Supplemental Figure 6b, $P = 0.76$). After this restricted test, animals were re-fed for one week, and then re-tested under sated conditions. Again, compared to consumption on the previous day, the number of test-day pellets consumed was reduced in *Drd1a-cre*$^{+}$, but not in *Drd1a-cre*$^{-}$ mice (Fig. 4c, $P = 0.039$ and $P = 0.73$ respectively). This suggests that inhibiting activity of prefrontal D1 neurons can attenuate food intake.

Downstream targets of mPFC stimulation

To identify the functional circuit that mediates this feeding behavior, we analyzed mPFC D1 neuronal projections. These could be readily visualized due to axonal localization of the ChR2-eYFP fusion protein in *Drd1a-cre*$^{+}$ animals. By combining tract-tracing with Fos responses following D1 stimulation, we surveyed the mouse brain for potential target regions. Animals were fiberoptically coupled to the laser, stimulated at 20 Hz and perfused 90 min later for detection of Fos expression. Axons of prefrontal D1 neurons were prominent in medial nucleus accumbens (shell and core), dorsomedial striatum, and caudal-medial, basolateral nucleus of the amygdala (mBLA, Fig. 5a, Supplemental Fig. 7a,b), and sparse axons were found in the lateral hypothalamus (Supplemental Fig. 7c). We found that Fos immunoreactivity was increased selectively in the mBLA of Cre+ animals, with the ipsilateral side showing significantly more Fos-positive nuclei than the contralateral side or *Drd1a-cre*$^{-}$ mBLA sections (Fig. 5b,c, $P = 0.003$). No differences in Fos were observed in the nucleus accumbens (Supplemental Figure 7d,e, $P = 0.35$). We characterized these mBLA, Fos-positive neurons using co-immunolabeling (Fig. 5d,e and Supplemental Figure 8), and found that ~85% of Fos-positive nuclei co-stained with CaMKII, a marker of glutamatergic neurons. This represented ~20% of CaMKII neurons within this region of the

mBLA. Only ~5% of Fos-positive nuclei were positive for parvalbumin (PV), a major type of interneuron in the mBLA (Fig. 5f).

To verify the presence of prefrontal D1 neuron-terminal synapses in the mBLA, we used a Cre-dependent AAV encoding an eGFP fluorophore fused to synaptobrevin (*AAV-EF1a-DIO-Synb-eGFP*), which selectively labels presynaptic vesicles of an infected neuron (Fig. 5g). The resulting fluorescence is highly punctate, and when injected into *Drd1a-cre*$^{+}$ mice, putative synaptic contacts were observed in the same mBLA region as observed with ChR2-EYFP expression (Fig. 5g). By co-staining, these puncta were in close apposition (< 5 microns) to CaMKII-positive cell bodies, consistent with a direct synaptic connection (Fig. 5h) that corroborates the increases in Fos immunoreactivity.

mBLA terminal stimulation of D1 neurons drives intake

To test whether prefrontal D1 projections to the mBLA are sufficient for the increase in feeding during prefrontal stimulation, we injected *AAV-EF1a-DIO-ChR2-eYFP* virus in the mPFC of *Drd1a-cre*$^{+}$ mice while implanting an optical fiber directed to the mBLA (Fig. 6a). This allowed selective photostimulation of the terminals of these prefrontal D1 afferents and evaluation of the contribution of this specific projection to the feeding response. Examining mBLA after photostimulation revealed a significant increase in Fos immunoreactivity compared to the unstimulated, contralateral side (Fig. 6b,c, $P = 0.008$). Using the overnight feeding paradigm, selective terminal stimulation of prefrontal D1 afferents in the mBLA increased responding only in *Drd1a-cre*$^{+}$ mice (Fig. 6d, $P = 0.007$), as measured by the ratio of ‘light’ to ‘no-light’ cumulative responses over the course of the 13-h session. This increase in responding resembled that seen with direct photostimulation of the PFC (Fig. 3g), although the ratio increased more quickly during the early hours of the test (3–6) and remained relatively constant after hour 7. Overall, *Drd1a-cre*$^{+}$ animals showed increased responses during the illuminated session ($P = 0.018$), while control animals showed no difference (Fig. 6e). Importantly, the *Drd1a-cre*$^{+}$ animals also showed a significant increase in intake, consuming ~0.6 g more food than control animals (Fig. 6f, $P = 0.021$). These results suggest that mPFC D1 terminal stimulation in mBLA is sufficient to drive intake. It is possible that these effects are due to antidromic activity in the mPFC, and while no Fos differences were seen between the ipsilateral and contralateral sides (Supplemental Fig. 9, $P = 0.53$), Fos assessment might not be sensitive enough to detect low levels of antidromic activity.

To experimentally verify the role of the mBLA in mediating this response, we additionally administered a halorhodopsin virus driven by the CaMKII promoter (*AAV-CaMKIIa-eNpHR3.0-EYFP*) into the mBLA of *Drd1a-cre*$^{+}$ mice prior to placement of the optical fiber. This allowed simultaneous stimulation of prefrontal D1 fiber terminals using blue light, and inhibition of CaMKII cell bodies in the mBLA using yellow light (Fig. 6g). Immunostaining revealed expression of halorhodopsin in the mBLA, with some expression also present in the central nucleus of the amygdala (Fig. 6h). Using the 1 h feeding paradigm, blue light alone was sufficient to increase intake, and this intake was reduced to baseline levels when blue and yellow light were contemporaneous (Fig. 6i, $P = 0.002$,), verifying that downstream activity of CaMKII neurons is necessary for the feeding response

and that the terminal stimulation results are not due to antidromic effects. Co-illumination of blue and yellow light did not change activity (Supplemental Fig. 10, $P = 0.759$). These results strongly suggest that prefrontal D1 neurons drive food intake via connections with mBLA.

DISCUSSION

In the present study we show that selectively stimulating prefrontal D1 neurons and their afferents within the BLA can increase feeding. This follows the observation that D1 neurons are activated during feeding, and provides functional data to support a direct role for D1 prefrontal neuron activity in intake. Notably, activation of these D1 neurons does not result in classical 'top-down inhibition' of behavior, but rather drives food intake in sated animals. In addition, stimulation of the prefrontal D1 neurons activates a subset of glutamatergic neurons in the BLA, and glutamatergic afferents from the BLA have been previously shown to be important for appetitive behaviors via interactions with the NAc[26], suggesting that cortical control of these neurons could modulate this appetitive drive. The BLA has also been implicated in other food seeking behaviors such as conditioned potentiation of feeding through its reciprocal connections back to the mPFC (27). Finally, these BLA glutamatergic neurons also project to the lateral hypothalamus, another structure important for both food intake and reward[27].

Prefrontal neurons also project to the shell region of the NAc[28], and interruption of glutamate signaling in the NAc shell has been shown to have strong effects on feeding[29]. The NAc receives glutamatergic input from a variety of nuclei, including the prefrontal cortex, and we show that projections from D1 neurons are also found there. However, we did not observe a Fos response in the NAc suggesting that, under the stimulation conditions used, the prefrontal D1 system is not directly influencing the NAc neuronal activity as assessed with Fos.

The sustained effect on feeding following prolonged stimulation periods is notable. We saw no changes in the first hour of photostimulation for either the PFC-targeted or BLA-targeted groups during the overnight feeding paradigm, but rather gradual increases during the subsequent hours. Because animals began the test during times when they would normally start feeding, the stimulation during the first hours could be obscured by normal intake (e.g. Supplemental Figure 4a,b). This suggests that only once satiety signals were present did prefrontal stimulation drive additional intake. This is further supported by the 1-hour free-feeding data, where increases were observed at times when animals do not typically eat, and thus are presumably sated. Also the observation that intake of both grain pellets and more palatable foods are increased as a result of stimulation suggests that palatability does not seem to play a significant role in this stimulated intake.

While we have implicated D1-receptor containing neurons in food intake, how dopamine interacts with these neurons to influence this response is not yet known. Dopamine in the PFC is increased during consumption of food[30], so increased firing of VTA neurons could provide increased activation of D1 neurons. It is possible that sustained increases in D1 activity are required for the feeding response, something that could occur with PFC over-

activation[4], as is seen in some obese humans. However, it is also possible that another common feature to D1 neurons could be mediating this, independent of dopamine. The increased intake here is nonetheless consistent with previous studies that demonstrate a relationship between dopamine and feeding in nigrostriatal and mesolimbic pathways[13].

A recent study has found support for a role of mPFC mu-opioid receptor (MOR) activity in mediating food intake, but the neuronal population responsible was not identified[9]. It is possible that these mu-opioid receptors are located on interneurons, whose inhibition results in a net disinhibition of glutamatergic neurons. However, recent work suggests that MOR and D1 co-localize in prefrontal neurons, and an interaction between the beta-gamma subunit of the MOR g-protein on adenylyl cyclase results in potentiation of D1 agonism[31]. While the present study identifies that D1 pyramidal neurons are candidates for mediating this effect, further work will need to examine the contribution of mu-opioids to D1-receptor cellular excitability through either direct or indirect mechanisms.

By selectively limiting our stimulation to the D1 neurons, we focus on a neuronal population that has been previously demonstrated to be necessary for working memory[17], interval timing[18], as well as relapse to palatable food seeking[22,23]. These results extend a role for D1 neurons in the feeding response, and suggest a direct interaction with the amygdala to mediate this effect. This circuit also presents new therapeutic opportunities, as future interventions for obesity or eating disorders may consider this prefrontal circuit for pharmacotherapy.

METHODS

Animals

Sixty-four D1-dopamine receptor Cre-recombinase male and female mice (*Drd1a-cre*$^{+}$ and *Drd1a-cre*$^{-}$ littermate controls, strain EY262, Gensat, backcrossed at least 10 generations to a C57Bl/6 background) weighing 20–30 g were used for these studies. For behavioral optogenetic studies, males were exclusively used. All animals were group-housed until optogenetic testing, when individuals were single-housed. Animals were on a 12 h light/dark cycle and provided standard chow and water *ad libitum* except during behavioral training described below, and all animal procedures were performed in accordance with the protocol approved by the Institutional Animal Care and Use Committee (IACUC).

Viral preparation and surgery

Viral production for the flox-channelrhodopsin *(AAV-EF1a-DIO-ChR2-eYFP*) and flox-eGFP-synaptobrevin (*AAV-EF1a-DIO-Synb-eGFP*) was accomplished using a triple-transfection, helper-free method, and purified as described in detail previously[33]. Additional ChR2, flox-eNpHR (*AAV-EF1a-DIO-eNpHR3.0-EYFP*), and CaMKII promoted eNpHR (*AAV-CaMKIIa-eNpHR3.0-EYFP*) virus were purchased from the UNC viral core. To generate the flox-eGFP-Synaptobrevin fusion construct, the flox-ChR2 construct was cut inside of the asymmetric loxP sites using NheI and AscI restriction enzymes, and a cassette containing synaptobrevin fused to eGFP was cloned in.

For surgery, animals were anesthetized with 10% ketamine/ 1% xylazine and placed in a stereotaxic frame (Stoelting). After craniotomy, mice were injected with AAV-flox-ChR2 or AAV-flox-eNpHR into the prefrontal cortex (AP: +1.8, ML –0.2, DV –2.8) and/or CaMKII promoted eNpHR mBLA (AP: –1.8. ML –3.0, DV –4.6), with immediate placement of an optical fiber cannula (200 μm core, 0.22NA, Doric Lenses) either into the prefrontal cortex at the same coordinates (unilateral or bilateral), or just dorsal to the caudo-medial basolateral amygdala (AP: –1.8, ML –3.0, DV –4.5). Animals receiving AAV-eGFP-synaptobrevin in the prefrontal cortex were not cannulated. The injection consisted of 0.5 microliter of approximately 10^{11} infectious particles per milliliter. Animals recovered for at least two weeks before behavioral or electrophysiological testing.

Electrophysiology

Brain slices were prepared as previously described[34]. Briefly, mice were anesthetized (chloral hydrate, 400 mg/kg IP) and brains removed and placed in ice-cold (4°C) artificial cerebrospinal fluid (ACSF) in which sucrose (252 mmol/L) was substituted for sodium chloride (sucrose-ACSF). Blocks of tissue containing prefrontal cortex (400 μm) were cut in sucrose-ACSF with an oscillating-blade tissue slicer (Leica). Slices were placed in a submerged recording chamber; bath temperature was then raised slowly to 32°C. The standard ACSF (pH 7.35), equilibrated with 95% oxygen/5% carbon dioxide, contained 128 mmol/L sodium chloride, 3 mmol/L potassium chloride, 2 mmol/L calcium chloride, 2 mmol/L magnesium sulfate, 24 mmol/L sodium bicarbonate, 1.25 mmol/L sodium phosphate, and 10 mmol/L d-glucose. There was recovery period of 1 to 2 hours before recording.

ChR2-positive pyramidal neurons in layer 5 were visualized by video microscopy using a microscope (60× infrared lens; Olympus, Center Valley Pennsylvania) with infrared differential interference contrast and an eYFP filter cube (Olympus). Patch pipettes (3–5 MΩ) were pulled from glass tubing using a Flaming-Brown Horizontal Puller (Sutter). The pipette solution contained the following: 115 mmol/L potassium gluconate, 5 mmol/L potassium chloride, 2 mmol/L magnesium chloride, 2 mmol/L magnesium adenosine triphosphate, 2 mmol/L disodium adenosine 5′-triphosphate, 10 mmol/L sodium-phosphocreatine, .4 mmol/L disodium guanosine 5′-triphosphate, and 10 mmol/L HEPES, pH 7.33 (American Bioanalytical). Neurobiotin (.3%; Vector Laboratories) was added to the pipette solution to mark selected cells for later processing and imaging.

Whole-cell recordings were with an Axoclamp-2B amplifier (Molecular Devices). The output signal was low-pass filtered at 3 kHz and digitized at 15 kHz; data were acquired by pClamp 9.2/Digidata 1320 software (Molecular Devices). Series resistance, which was monitored throughout the experiment, was usually between 4 and 8 MΩ. Postsynaptic currents were studied in the continuous single-electrode voltage-clamp mode (3000 Hz low-pass filter) clamped near resting potential (75 mV ± 5 mV). Photostimulation of the slice was performed using a 100 mW, 473 nm laser (OEM optics) driven at 20 Hz by an interval generator (pulsewidth 10 ms). The fiberoptic was placed just above the slice, outside of the perfusion solution.

Food deprivation/refeeding paradigm

Animals were designated to deprived or control groups, and the deprived animals' food was removed at 2:00 pm. Twenty-four hours later, both control and deprived groups were given several small chow pellets in the home cage, and the deprived animals additionally received food in the metal hopper cage-top. After 90 m, food was weighed and animals were immediately intracardially perfused and prepared for immunohistochemistry (see below).

One-hour free-feeding photostimulation paradigm

After recovery from surgery, animals were placed into a home-cage that lacked bedding, but contained a small weigh-boat containing grain pellets. Animals habituated to the home-cage 1h a day for three days prior to photo-illumination. On day 4, animals were briefly anesthetized using isoflurane, and the incoming fiberoptic was joined to the indwelling optical fiber. The animal was placed in the home-cage and photoillumination took place in 10 repeating cycles of 3 min, 20 Hz light pulses (pulsewidth 10 msec) and 3 min no illumination (1 h). Pellets were counted at the end of the test, and subtracted from the initial amount. After several days of recovery, animals were again tested using 5 Hz light pulses. For the PFC D1 terminal/mBLA stimulation/inhibition experiment, 20Hz blue light was delivered simultaneously with virtually constant yellow (590 nm, 2900ms on, 100 ms off) light from a separate source laser (OEM) using the same 3 min on/off cycling protocol. For the high-fat experiment, animals were exposed to the high-fat diet in their home-cage several days prior to testing. On test-day, a high-fat pellet was placed in the testing home-cage, and the same protocol was used, with stimulation at 20 Hz.

One-hour free-feeding photoinhibition paradigm

After recovery from surgery, animals were food restricted to ~90% of free-feeding weight and habituated to the home-cage as described above for 4 days. On the 'restricted' test day, light delivery consisted of four, 15 minute epochs as follows: No light, yellow light, no light, yellow light. Yellow light was nearly constant (2900ms on, 100 ms off) during illuminated epochs. During each change in light, pellets were counted and subtracted from the previous amount to calculate amounts eaten during light and no light epochs. After testing, animals were fed *ad libitum* for 1 wk, and then tested again fully sated. For this test, the light epochs were reversed such that yellow light was presented first. Pellets were counted at the end of the session, and compared to a pre-test session the day before where there was no illumination.

Overnight feeding paradigm

After recovery from surgery, animals were food restricted to 85–90% of free-feeding weight. Following three nights of food restriction, animals were trained to make an operant response for a grain pellet (20 mg, BioServ) on a cued, fixed response 1 schedule in an apparatus (Med Associates) that had a nose-poke on one side and a food magazine on the other. After animals reached asymptotic responding (at least 80 pellets in 1 hour for 2 days), animals were returned to *ad-libitum* in their home cages for at least one week until weights recovered to pre-restriction amounts. On test day, animals were taken to the testing apparatus, briefly anesthetized using isoflurane, and the incoming fiberoptic was joined to

the indwelling optical fiber. The animal was then placed in the apparatus and the overnight feeding program was initiated. This program consisted of repeating, 1 h cycles consisting of 2, 30 min epochs starting at 5:30 pm, 1.5 h before the onset of the dark cycle. In the first 30 min epoch, the laser was off, and no light was delivered to the animal. In the second 30 min epoch, 5 three-minute, 20 Hz light trains were delivered interspersed with three minutes of no laser (see Figure 3e for schematic). Throughout the test, animals receive a grain pellet after a nose-poke (response). Importantly, after the first response the cue light was turned off and remained off, so there were no cues associated with the response. Animals performed the test for 13 hours, and after the animal was removed from the apparatus in the morning, the number of pellets remaining were counted and subtracted from the total to give the exact number of pellets consumed. Animals in the high fat overnight feeding paradigm were not restricted, and placed in the chamber after laser coupling with 2 high fat pellets (~ 6.5–8 g total). Licks on a water spout and non-reinforced head entries were measured over the 13 hours, and initial and final weight of food was recorded.

Immunofluorescence

All animals that performed behavioral tests were briefly anesthetized with isoflurane, coupled to the laser, and placed back their home cage. After anesthetic recovery, light was delivered at 20 Hz for 5 min, in 30 s on/off trains. 90 min after the start of light delivery, animals were deeply anesthetized and intracardially perfused with 4% paraformaldehyde. The brain was removed and post-fixed in paraformaldehyde, and after immersion in sucrose for cryoprotection, 40 μm sections were made on a freezing microtome, and stored in 1× PBS with 0.01% sodium azide to prevent bacterial growth. Immunohistochemistry was performed according to methods described previously (19). Staining for Fos (Rabbit anti-cFos; Santa Cruz-sc-52; 1:500), CaMKII (Mouse anti-camkii; Cayman Chemical-10011437; 1:250), PV (Mouse anti-parvalbumin; Swant-PV 235; 1:1000), Cre (Mouse anti-Cre; Millipore-MAB 3120; 1:500), or D1-receptor (Guinea Pig anti-D1R; Frontier Science co-D1R-GP-Af500; 1:200) with secondary antibodies (Alexa 488 or 555; Invitrogen/Life Sciences- A21202, A31570, A31572; Jackson Immunoresearch- 706-546-148, 1:500;) was performed in 3% normal donkey serum and 0.3% Triton-X 100. Tissue was visualized and images were captured using a fluorescent microscope (Zeiss) using standard FITC and TRITC filters or using a confocal microscope (Olympus). Fos labeling was quantified by standard threshold settings in ImageJ (NIH) over matched areas on one or more (averaged) sections per animal, and overlap between Fos, PV, CaMKII, D1, and/or Cre was determined by apposition of the separate color channels.

Statistics

No statistical methods were used to predetermine sample sizes but our sample sizes are similar to those reported in previous publications[19,35]. Cage littermates were assigned to experimental or control groups based on genotype, and were age- and weight-matched. Data distribution was assumed to be normal but this was not formally tested. Comparisons were made between *Drd1a-cre*$^{+}$ and *Drd1a-cre*$^{-}$ animals using 1-way and 2-way ANOVA (with light, genotype, side of injection and/or time as factors) or unpaired, two-tailed t-tests for pellet consumption, and within subjects using paired, two-tailed t-tests when appropriate.

Differences in means were considered significant if they were less than $P = 0.05$, and were calculated using Graphpad Prism 5.0 and 6.0. Error bars represent s.e.m.

Supplementary Material

Refer to Web version on PubMed Central for supplementary material.

Acknowledgements

We thank Xue Sun and Cali Calarco for experimental assistance. This work was supported by R01DK098994 (RJD), F32DK091172 and RL5DA024858 (BBL), and the State of Connecticut, Department of Mental Health and Addiction Services (RJD).

References

1. Rangel A, Camerer C, Montague PR. A framework for studying the neurobiology of value-based decision making. Nat. Rev. Neurosci. 2008; 9:545–556. [PubMed: 18545266]
2. Miller EK, Cohen JD. An integrative theory of prefrontal cortex function. Annu. Rev. Neurosci. 2001; 24:176–202.
3. Ikeda M, Brown J, Holland AJ, Fukuhara R, Hodges JR. Changes in appetite, food preference, and eating habits in frontotemporal dementia and Alzheimer's disease. J. Neurol. Neurosurg. Psychiatr. 2002; 73:371–376. [PubMed: 12235302]
4. Ochner CN, Green D, van Steenburgh JJ, Kounios J, Lowe MR. Asymmetric prefrontal cortex activation in relation to markers of overeating in obese humans. Appetite. 2009; 53:44–49. [PubMed: 19426775]
5. de Araujo IE, Rolls E, Kringelbach M, Mcglone F, Phillips N. Taste-olfactory convergence, and the representation of the pleasantness of flavour, in the human brain. Eur. J. Neurosci. 2003; 18:2059–2068. [PubMed: 14622239]
6. Kolb B, Nonneman AJ. Prefrontal cortex and the regulation of food intake in the rat. J Comp. Physiol. Psychol. 1975; 88:806–815. [PubMed: 1056942]
7. Wolf-Jurewicz K. The role of the medial prefrontal cortex in food intake in dogs. Acta Physiol. Pol. 1982; 33:393–401. [PubMed: 6964027]
8. Davidson TL, et al. Contributions of the hippocampus and medial prefrontal cortex to energy and body weight regulation. Hippocampus. 2009; 19:35–52.
9. Mena JD, Sadeghian K, Baldo B. Induction of Hyperphagia and Carbohydrate Intake by {micro}-Opioid Receptor Stimulation in Circumscribed Regions of Frontal Cortex. J. Neurosci. 2011; 31:3249–3260. [PubMed: 21368037]
10. Hnasko TS, Sotak BN, Palmiter RD. Morphine reward in dopamine-deficient mice. Nature. 2005; 438:854–857. [PubMed: 16341013]
11. Dileone RJ, Taylor JR, Picciotto MR. The drive to eat: comparisons and distinctions between mechanisms of food reward and drug addiction. Nat. Neuro. 2012; 15:1330–1335.
12. Narayanan NS, Guarnieri DJ, DiLeone RJ. Metabolic hormones, dopamine circuits, and feeding. Front. Neuroendocrinol. 2010; 31:104–112. [PubMed: 19836414]
13. Hnasko TS, et al. Cre recombinase-mediated restoration of nigrostriatal dopamine in dopamine-deficient mice reverses hypophagia and bradykinesia. Proc. Natl. Acad. Sci. USA. 2006; 103:8858–8863. [PubMed: 16723393]
14. Johnson PM, Kenny PJ. Dopamine D2 receptors in addiction-like reward dysfunction and compulsive eating in obese rats. Nat. Neurosci. 2010; 13:635–641. [PubMed: 20348917]
15. Hommel JD, et al. Leptin receptor signaling in midbrain dopamine neurons regulates feeding. Neuron. 2006; 51:801–810. [PubMed: 16982424]
16. Hernandez L, Hoebel BG. Feeding and hypothalamic stimulation increase dopamine turnover in the accumbens. Physiol. Behav. 1988; 44:599–606. [PubMed: 3237847]

17. Chaudhury D, et al. Rapid regulation of depression-related behaviours by control of midbrain dopamine neurons. Nature. (epub ahead of print, 2013).
18. Castner SA, Williams GV, Goldman-Rakic PS. Reversal of antipsychotic-induced working memory deficits by short-term dopamine D1 receptor stimulation. Science. 2000; 287:2020–2022. [PubMed: 10720329]
19. Narayanan NS, Land BB, Solder JE, Deisseroth K, DiLeone RJ. Prefrontal D1 dopamine signaling is required for temporal control. Proc. Natl. Acad. Sci. USA. 2012; 109:20726–20731. [PubMed: 23185016]
20. Hitchcott PK, Quinn JJ, Taylor JR. Bidirectional modulation of goal-directed actions by prefrontal cortical dopamine. Cereb. Cortex. 2007; 17:2820–2827. [PubMed: 17322558]
21. Gaspar P, Bloch B, Le Moine C. D1 and D2 receptor gene expression in rat frontal cortex: cellular localization in different classes of efferent neurons. Eur. J. Neurosci. 1995; 7:1050–1063. [PubMed: 7613610]
22. Nair SG, et al. Role of dorsal medial prefrontal cortex dopamine D1-family receptors in relapse to high-fat food seeking induced by the anxiogenic drug yohimbine. Neuropsychopharmacology. 2011; 36:497–510. [PubMed: 20962767]
23. Touzani K, Bodnar RJ, Sclafani A. Acquisition of glucose-conditioned flavor preference requires the activation of dopamine D1-like receptors within the medial prefrontal cortex in rats. Neurobiol. Learn. Mem. 2010; 94:214–219. [PubMed: 20566378]
24. Cardin JA, et al. Targeted optogenetic stimulation and recording of neurons in vivo using cell-type-specific expression of Channelrhodopsin-2. Nat. Protoc. 2010; 5:247–254. [PubMed: 20134425]
25. Seong HJ, Carter AG. D1 receptor modulation of action potential firing in a subpopulation of layer 5 pyramidal neurons in the prefrontal cortex. J. Neurosci. 2012; 32:10516–10521. [PubMed: 22855801]
26. Stuber GD, et al. Excitatory transmission from the amygdala to nucleus accumbens facilitates reward seeking. Nature. 2011; 475:377–380. [PubMed: 21716290]
27. Petrovich GD, Holland PC, Gallagher M. Amygdalar and prefrontal pathways to the lateral hypothalamus are activated by a learned cue that stimulates eating. J. Neurosci. 2005; 25:8295–8302. [PubMed: 16148237]
28. Gabbott PL, Warner TA, Jays PR, Salway P, Busby SJ. Prefrontal cortex in the rat: projections to subcortical autonomic, motor, and limbic centers. J. Comp. Neurol. 2005; 492:145–177. [PubMed: 16196030]
29. Maldonado-Irizarry CS, Swanson CJ, Kelley AE. Glutamate receptors in the nucleus accumbens shell control feeding behavior via the lateral hypothalamus. J. Neurosci. 1995; 15:6779–6788. [PubMed: 7472436]
30. Bassareo V, Di Chiara G. Differential influence of associative and nonassociative learning mechanisms on the responsiveness of prefrontal and accumbal dopamine transmission to food stimuli in rats fed ad libitum. J. Neurosci. 1997; 17:851–861. [PubMed: 8987806]
31. Olianas MC, Dedoni S, Onali P. Potentiation of dopamine D1-like receptor signaling by concomitant activation of δ- and μ-opioid receptors in mouse medial prefrontal cortex. Neurochem. Int. 2012; 61:1404–1416. [PubMed: 23073238]
32. Paxinos, G.; Franklin, KBJ. The mouse brain in stereotaxic coordinates. USA: Elsevier; 2004.
33. Hommel JD, Sears RM, Georgescu D, Simmons DL, DiLeone RJ. Local gene knockdown in the brain using viral-mediated RNA interference. Nat. Med. 2003; 9:1539–1544. [PubMed: 14634645]
34. Li N, et al. Glutamate N-methyl-D-aspartate receptor antagonists rapidly reverse behavioral and synaptic deficits caused by chronic stress exposure. Biol. Psychiatry. 2011; 69:754–761. [PubMed: 21292242]

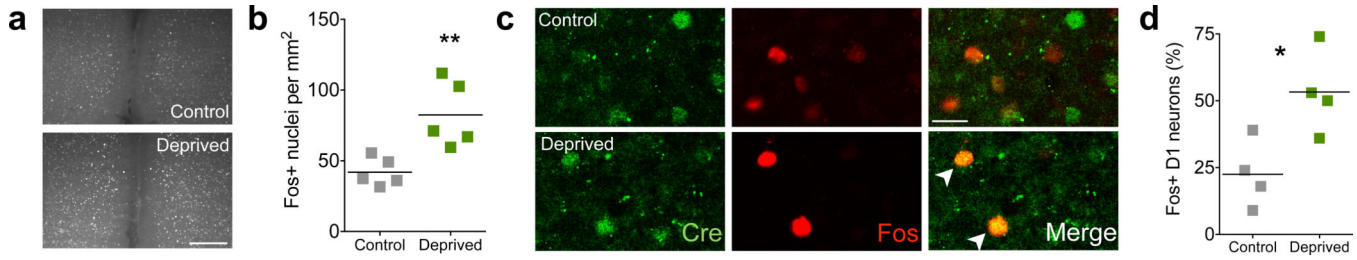

Figure 1.

Characterization of prefrontal neurons activated during feeding. (**a**) Representative micrographs showing prefrontal Fos nuclei in control and deprived *Drd1a-cre*$^{+}$ mice after 90 m access to food (scale bar = 200 μm). (**b**) Quantification of Fos positive nuclei in the prefrontal cortex of control and deprived/re-fed animals (n = 5,5 animals, t_8 = 3.6, P = 0.007, 2-tailed t-test; control = 51.6± 5.1; deprived = 101.4± 12.3, mean ± s.e.m.). (**c**) Representative single channel and overlay confocal micrographs of Cre (green) and Fos (red) for control and deprived mice. Note examples of overlap (white arrowheads) in the deprived condition (scale bar = 20 μm). (**d**) Quantification of the percentage of *Drd1a-cre*$^{+}$ nuclei that were also Fos positive (n = 4,4 animals, t_6 = 3.1, P = 0.022, 2-tailed t-test; control = 22.5± 6.5; deprived = 53.3± 7.8, mean ± s.e.m.). * P < 0.05, ** P < 0.01.

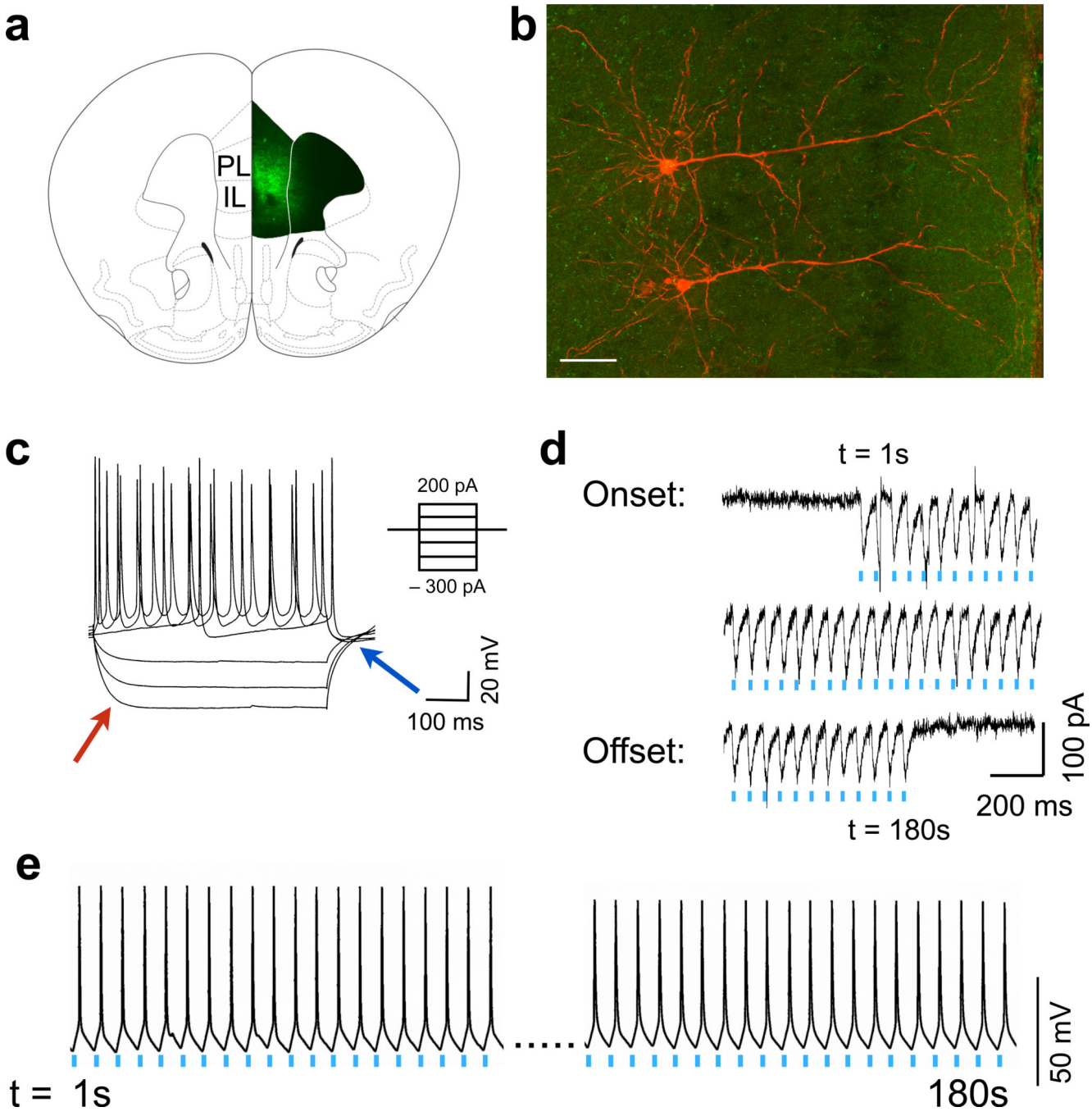

Figure 2.

Physiological responses to prefrontal D1 photoactivation. (**a**) ChR2 expression in prefrontal D1 neurons after viral injection in *Drd1a-cre*$^{+}$ mice. Strong staining is seen in layer 2/3 and layer 5 of both the prelimbic (PL) and infralimbic (IL) prefrontal cortex. (**b**) Representative micrograph of two D1 positive layer 5 pyramidal neurons filled with biotin (red; background eYFP in green, scale bar = 60 μm). (**c**) Physiological properties of a D1 neuron in response to depolarizing and hyperpolarizing currents. Note a lack of voltage sag (red arrow) or rebound depolarization (blue). (**d**) Inward currents induced by 20 Hz blue light demonstrates

high fidelity over the course of 3 m. (**e**) Representative voltage trace showing high fidelity action potentials in response to 20 Hz blue light over the course of 3 m.

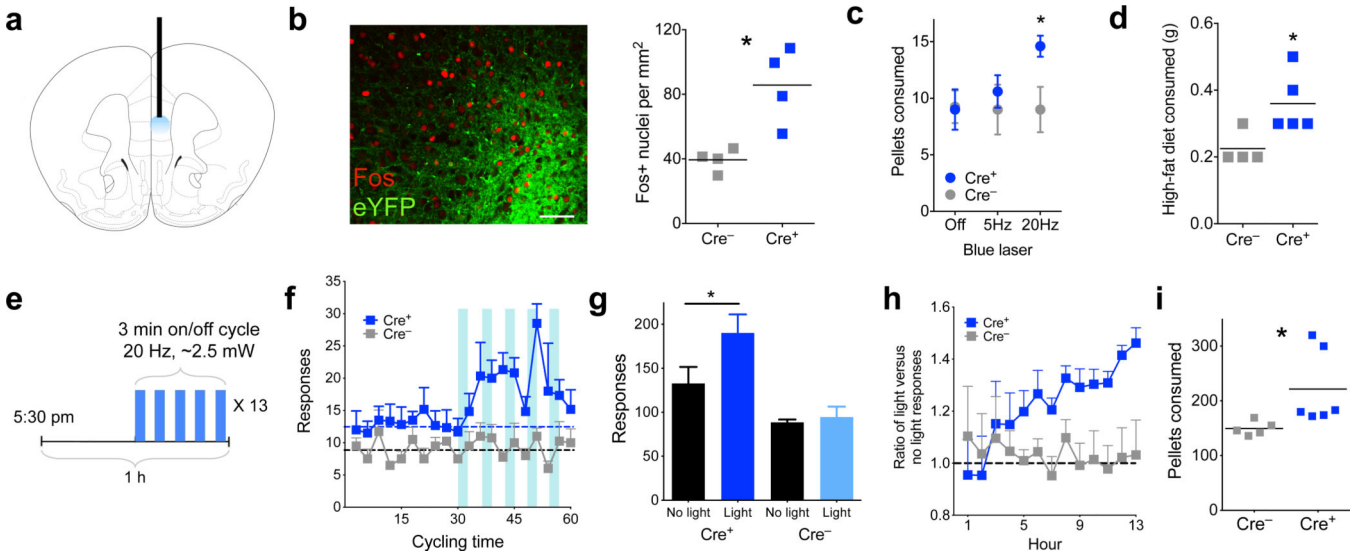

Figure 3.

Prefrontal D1 photostimulation leads to increased food intake. (**a**) Schematic showing placement of optical fiber within medial prefrontal cortex. (**b**) Left, confocal micrograph showing dense eYFP expression in layer 5 (green), along with Fos (red, scale bar = 60 μm). Right, quantification of Fos+ nuclei in the mPFC of *Drd1a-cre*$^{+}$ and *Drd1a-cre*$^{-}$ animals after photostimulation (n = 4,4 animals, t_6 = 3.8, P = 0.01, 2-tailed t-test; Cre– = 30.5± 2.7; Cre+ = 66.25± 9.1, mean ± s.e.m.). (**c**) Number of grain pellets consumed in 1 h with no photostimulation, 5 Hz, or 20 Hz stimulation (n = 4,5 animals, 20 Hz t_7 = 2.7, P = 0.029, 2-tailed t-test; 5 Hz t_7 = 0.6, P = 0.55, 2-tailed t-test). (**d**) Amount, in grams, of high-fat (45%) chow consumed in 1 h with 20Hz photostimulation (n = 4,5 animals, t_7 = 2.7, P = 0.032, 2-tailed t-test; Cre– = 0.23± 0.03; Cre+ = 0.36± 0.04, mean ± s.e.m.). (**e**) Schematic describing the overnight feeding paradigm. Thirteen 1 h cycles are divided into ‘no light’ and ‘light’ epochs. (**f**) Histogram of responding in *Drd1a-cre*$^{+}$ and *Drd1a-cre*$^{-}$ animals over the thirteen 1 h cycles, summated and overlayed onto 1 hour. Dashed lines represent average responses during ‘no light’ epoch (n = 6,4 animals $F_{(1,8)}$ = 7.6, P = 0.025, 2-way ANOVA, main effect of genotype). (**g**) Total number of responses in ‘light’ and ‘no light’ epochs over the 13 h test in *Drd1a-cre*$^{+}$ and *Drd1a-cre*$^{-}$ animals (n = 6,4, t_5 = 9.2, P = 0.0003, 2-tailed, paired t-test, overall interaction of genotype × light, $F_{(1,8)}$ = 14.2, P = 0.006, 2-way ANOVA. (**h**) Response ratio over 13 hours of cumulative ‘light’ divided by ‘no light’ responses. Values over 1.0 (dashed line) represent more responding during the ‘light’ epoch (n = 6,5 animals, $F_{(12,108)}$ = 1.9, P = 0.04, 2-way ANOVA, interaction of hour × genotype). (**i**) Total number of grain pellets consumed overnight in *Drd1a-cre*$^{+}$ and *Drd1a-cre*$^{-}$ animals (n = 6,5 animals, t_9 = 2.3, P = 0.049, 2-tailed t-test; Cre– = 149.6± 5.8; Cre+ = 221.5± 28.2, mean ± s.e.m.). Graphs represent mean ± s.e.m. * P < 0.05.

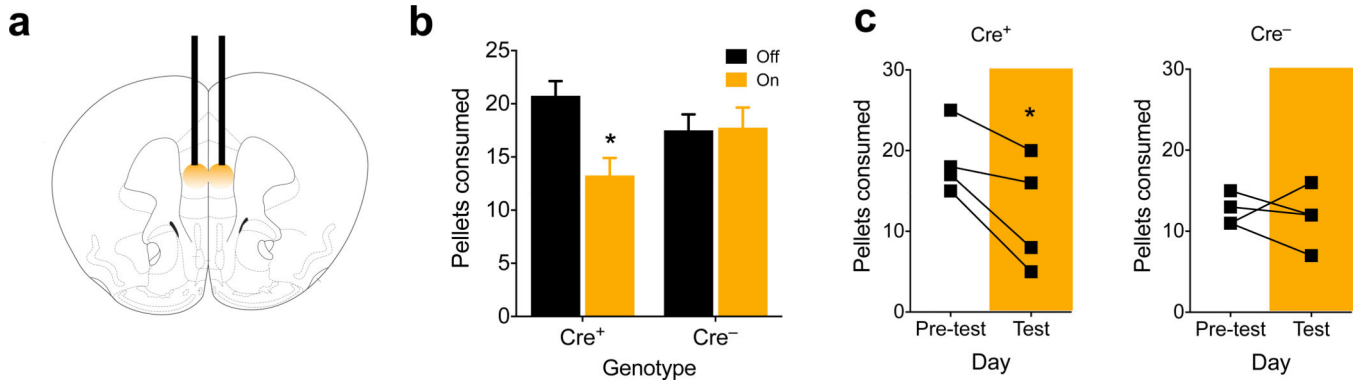

Figure 4.

Photoinhibition of prefrontal D1 neurons reduces food intake. (**a**) Schematic showing placement of bilateral optical fibers within the mPFC. (**b**) Number of pellets consumed in 1 h during light on and light off periods for food restricted *Drd1a-cre*$^{+}$ and *Drd1a-cre*$^{-}$ animals (n = 4,4 animals, t_3 = 3.3, P = 0.045, 2-tailed, paired t-test; overall interaction of light × genotype, $F_{(1,12)}$ = 5.8, P = 0.034, 2-way ANOVA. (**c**) Number of pellets consumed on the pre-test and test (photoinhibition) days for *ad-lib* fed *Drd1a-cre*$^{+}$ and *Drd1a-cre*$^{-}$ animals (n = 4,4 animals, Cre+ t_3 = 3.5, P = 0.039, 2-tailed, paired t-test; Cre– t_3 = 0.4, P = 0.73, 2-tailed, paired t-test; Cre+ pre-test = 18.8± 2.2, test = 12.3± 3.5; Cre– pre-test = 12.5± 1.0, test = 11.8± 1.8, mean ± s.e.m.). Graphs represent mean ± s.e.m. * P < 0.05.

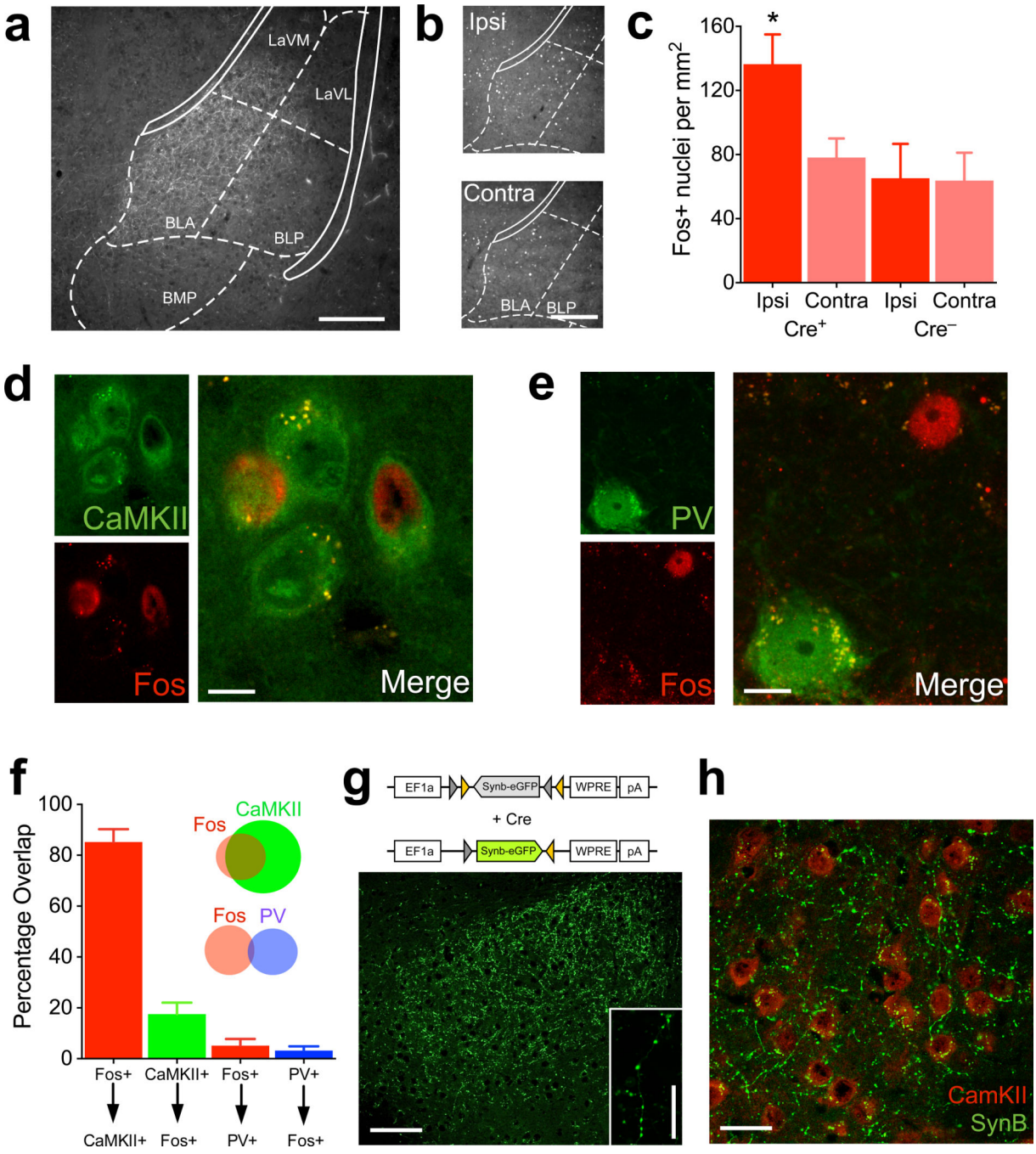

Figure 5.

Prefrontal D1 neurons project to and activate the medial basolateral amygdala. (**a**) Representative micrograph of eYFP/ChR2-positive axons of D1 PFC neurons in the BLA. Overlay from corresponding coronal slice in mouse brain atlas[32] (scale bar = 250μm). (**b**) Fos immunofluorescence on the ipsilateral (ipsi) and contralateral (contra) BLA of a *Drd1a-cre*$^{+}$ animal 90 min after photostimulation (scale bar = 250μm). (**c**) Quantification of Fos immunofluorescence on the ipsilateral and contralateral BLA of *Drd1a-cre*$^{+}$ and *Drd1a-cre*$^{-}$ animals 90 min after photostimulation (n = 6,4 animals, interaction between genotype ×

side, $F_{(1,8)} = 17.1$, $P = 0.003$, 2-way ANOVA). (**d**) Representative single channel and overlay micrographs demonstrating co-staining of Fos and CaMKII, a marker for glutamatergic neurons (scale bar = 10μm). (**e**) Representative single channel and overlay micrographs showing lack of overlap between Fos and parvalbumin (PV, scale bar = 10μm). (**f**) Quantification of overlap between Fos and CaMKII and PV. X-axis refers to the percentage of above-arrow positive neurons that are also below-arrow positive. Inset: Venn diagram visually depicting the amount of overlap between the two neuronal types with Fos (not to scale; $n = 3$). (**g**) Above, AAV construct for flox-eGFP-synaptobrevin fusion. Below, Micrograph showing eGFP labeled, pre-synaptic terminals in the BLA following PFC viral infusion into *Drd1a-cre*$^{+}$ mice (scale bar = 100μm). Inset: High-magnification showing synaptic boutons (scale bar = 18μm). (**h**) Micrograph of D1 PFC neuron terminals (green) with CaMKII immunodetection (red), demonstrating close apposition between the two (scale bar = 30μm). Graphs represent mean ± s.e.m. * $P < 0.05$. BLA- Basolateral amygdala-anterior, BLP- Basolateral amygdala-posterior, BMP- Basomedial amygdala, LaVL- Lateral amygdala-ventrolateral, LaVM-Lateral amygdala, ventromedial.

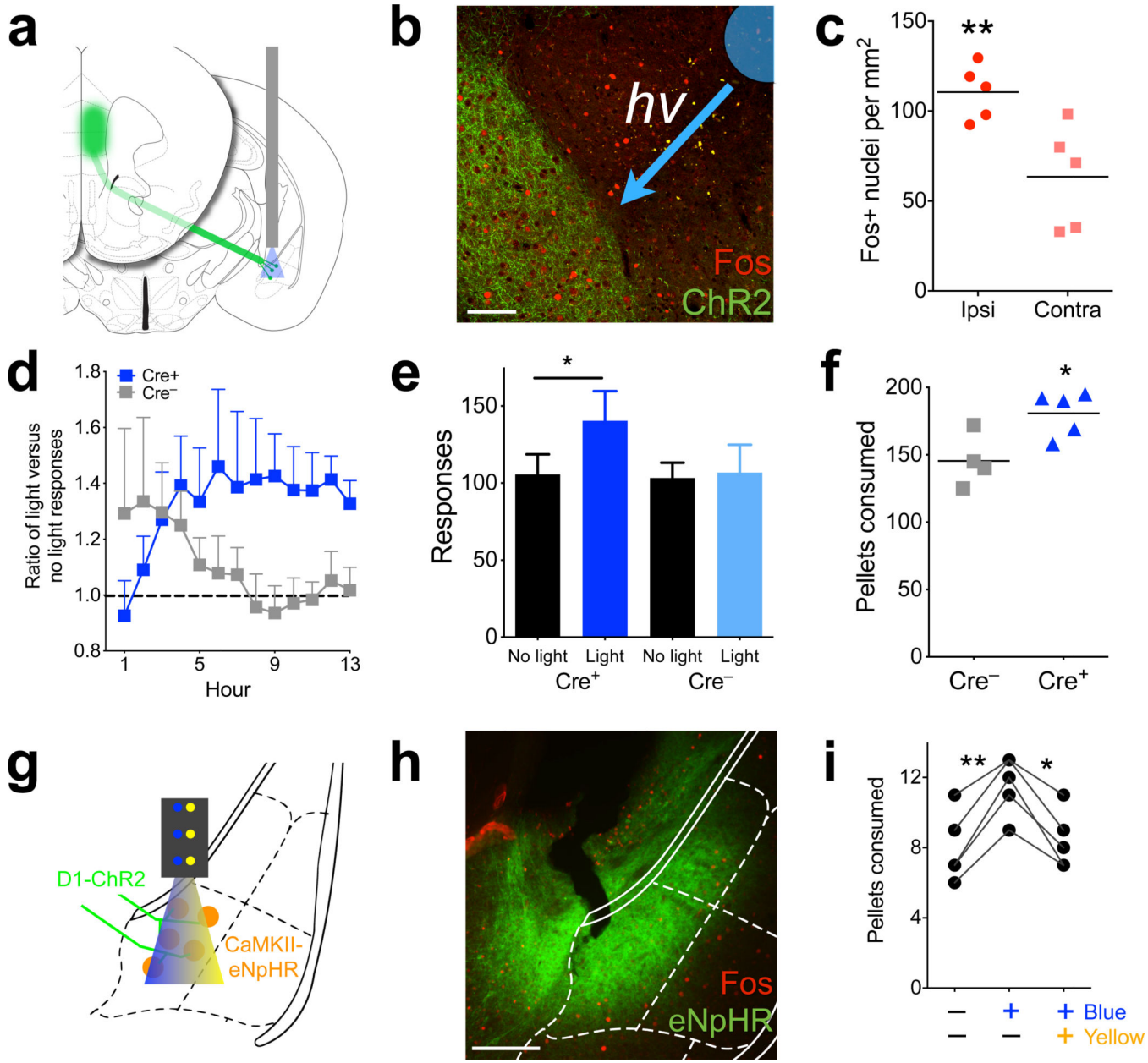

Figure 6.

Photostimulation of prefrontal D1 terminals in the mBLA increases intake. (**a**) Schematic representing the terminal targeting and photostimulation. (**b**) Micrograph depicting Fos in the D1-prefrontal terminal region of the mBLA in a *Drd1a-cre*$^{+}$ animal. Overlay depicts cannula tip and direction of incoming blue light (scale bar = 100μm). (**c**) Quantification of Fos in *Drd1a-cre*$^{+}$, mBLA targeted photostimulation, showing that light increases Fos (n = 5 animals, t_4 = 4.9, P = 0.008, 2-tailed, paired t-test; Ipsi = 20.6± 3.2; Contra = 11.8± 3.5, mean ± s.e.m.). (**d**) Response ratio of 'light' divided by 'no light' cumulative responses in *Drd1a-cre*$^{+}$ and *Drd1a-cre*$^{-}$ mice. Values over 1.0 (dashed line) represent more responding during the 'light' epoch (n = 5,4 animals, overall interaction of genotype × time, $F_{(1,12)}$ = 2.5, P = 0.007, 2-way ANOVA). (**e**) Total number of responses over the 13 hour test in

Drd1a-cre^{+} and *Drd1a-cre*$^{-}$ animals (n = 5,4 animals, t_7 = 3.9, P = 0.018, 2-tailed, paired t-test; overall interaction of genotype × light, $F_{(1,7)}$ = 5.7, P = 0.048, 2-way ANOVA). (**f**) Total number of grain pellets consumed in *Drd1a-cre*$^{+}$ and *Drd1a-cre*$^{-}$ animals (n = 5,4 animals, t_7 = 2.8, P = 0.021, 2-tailed t-test; Cre– = 152.0± 7.0; Cre+ = 180.8± 7.3, mean ± s.e.m.). (**g**) Schematic depicting incoming ChR2 axons from D1 neurons of the PFC, expression of CaMKII-promoted eNpHR in mBLA neurons, and fiberoptic cannula delivering both blue and yellow light to the region. (**h**) Representative micrograph showing eNpHR in the mBLA and CeA. (**i**) Number of pellets consumed in 1 h by *Drd1a-cre*$^{+}$ animals with prefrontal ChR2 and mBLA eNpHR, during no stimulation, blue light only, and blue and yellow light simultaneously (n = 5 animals, $F_{(2,8)}$ = 35.1, P = 0.002, One-way ANOVA, Bonferroni post-hoc). Graphs represent mean ± s.e.m. * P < 0.05, ** P < 0.01.